# Computational and Experimental Studies of Pressure Relief Doors in Ventilated Nacelle Compartments

Mr Peter Pratt, Dr. John Watterson, Dr. Emmanuel Benard
School of Aeronautical Engineering

*The Queen's University of Belfast, Belfast, Northern Ireland, BT9 5AG*
Email: p.pratt@qub.ac.uk; j.watterson@qub.ac.uk; e.benard@qub.ac.uk

**Keywords:** discharge flow, transonic, flapped outlet, vortices, oblique jets, shear layers

## Abstract:

A computational study of the performance of a flapped exhaust outlet is carried out. The outlet duct is curved, turning exhaust gases through 90$^o$ to the stream-wise direction before passing to the free-stream, and is of a rectangular cross section. A flap is fixed at the upstream edge. The resulting flow is a complex mixture of a jet emerging into a transonic flow, longitudinal vortices, free shear layers and normal shockwaves. The effect of varying flap angle, pressure ratio and free-stream Mach number is considered and force and discharge characteristics predicted. Information obtained is used to aid the design of a transonic wind tunnel test rig for gathering experimental data useful in the design of Pressure Relief Doors for ventilating engine nacelle compartments.

## Introduction

Performance and reliability of modern aircraft engines is affected by many factors, among which is the requirement for dedicated auxiliary air systems necessary for the safe and successful operation of the engine. An important set of auxiliary outlets are related to the relief of under cowl pressure in the event of a leak from, or burst of, high pressure supply lines to engine subsystems. These outlets are known as Pressure Relief Doors (PRDs) and are important to regulate excess internal pressure so as to prevent structural damage or failure.

One design for a PRD is a flap hinged at the downstream edge of the outlet. This flap will automatically open before the under cowl pressure reaches a structurally unsafe level, venting excess air to the free-stream. When the slender bodied flap enters the free-stream it creates a complex three dimensional (3D) flow structure which is a combination of longitudinal vortices, shear layers, an oblique jet and in some cases normal shockwaves. The exact combination and development of these structures is dependent on flap geometry, flap angle, free-stream Mach number and the ratio of under cowl to free-stream total pressures.

The design of such a system requires reliable information on force and discharge characteristics across a range of parameters. Very little research has been done on this subject, especially in recent years. Consequently a conservative approach to design has been adopted by the aerospace industry and more detailed information is now required to achieve an efficient design that satisfies both customers and certification authorities.

It is proposed that, through the use of a systematic process of computational investigations and experimental studies, a design database can be developed to help improve aerodynamic and structural performance of PRDs.

## Literature

Current PRD designs are based on literature regarding the discharge of auxiliary outlets to transonic free-stream flows. There are a number of passing mentions of experimental studies[1,2] specifically related to flapped outlets in papers concerning more generalised auxiliary air systems. However the most comprehensive set of experimental data is presented by Vick[3] in NACA TN4007. This deals with force and discharge characteristics of flapped, curved duct outlets in transonic flows and has particular relevance and influence on current PRD designs. Information on the performance of inclined auxiliary outlets is found in studies by Dewey[4] and Vick[5], with these showing that the discharge performance for given flow conditions is better for outlets with flaps than without.

While the information presented in NACA TN4007 is of great importance, it raises a number of questions and covers only a small range of parameters. There is no consideration of the flow structures formed around or downstream of the outlet and therefore no satisfactory explanation of the effect of flap angle, geometry, pressure ratio or free-stream Mach number on the discharge performance of the outlet.

For an efficient design of a PRD it is important however to understand how the above-mentioned parameters effect the flow field and therefore the discharge and force characteristics.

## Methodology

The expensive nature of high-speed wind tunnel experiments means that to cover a wide range of design parameters a computational model is preferable. However experimental data is still required to validate any numerical solutions. A flapped outlet above a plenum chamber should be used to simulate the PRD system rather than the ducted outlets found in the literature. A lack of description of, or explanation for, the flow physics of flapped outlets within previous literature raises questions with regard to the scale lengths and properties of any flow structures. This leads therefore to uncertainties when considering the design of a suitable test rig and its related instrumentation. A numerical study of the experiment described in NACA TN4007 was therefore proposed, with the predictions of the computational model being compared to the published data to provide a greater understanding of the physics of the flow field. This in turn allowed for a validation of a numerical model, which can be used to help design the experimental test rig. The commercial CFD package, Fluent 6$^{TM}$, was used for the calculations.

The computational domain was based on the geometry of the wind tunnel and flapped outlet used in the NACA experimental study, as shown in figure 1 and figure 2. The outlet consists of a rectangular duct 1″ wide by 1.865″ in length, which turns the exhaust flow through 90° about a radius of curvature of 2″ into the streamwise direction. The upstream edge of the orifice is extended 0.375″ so that the orifice length is 1.49″. A flat, rectangular flap 1″ wide by 1″ long and 0.032” thick is attached to the upstream edge of the duct orifice. The orifice leading edge was placed 8″ downstream of the inflow boundary. With the computational domain being symmetric, only one half, measuring 17″ long by 3.125″ wide by 4.5″ tall was modelled.

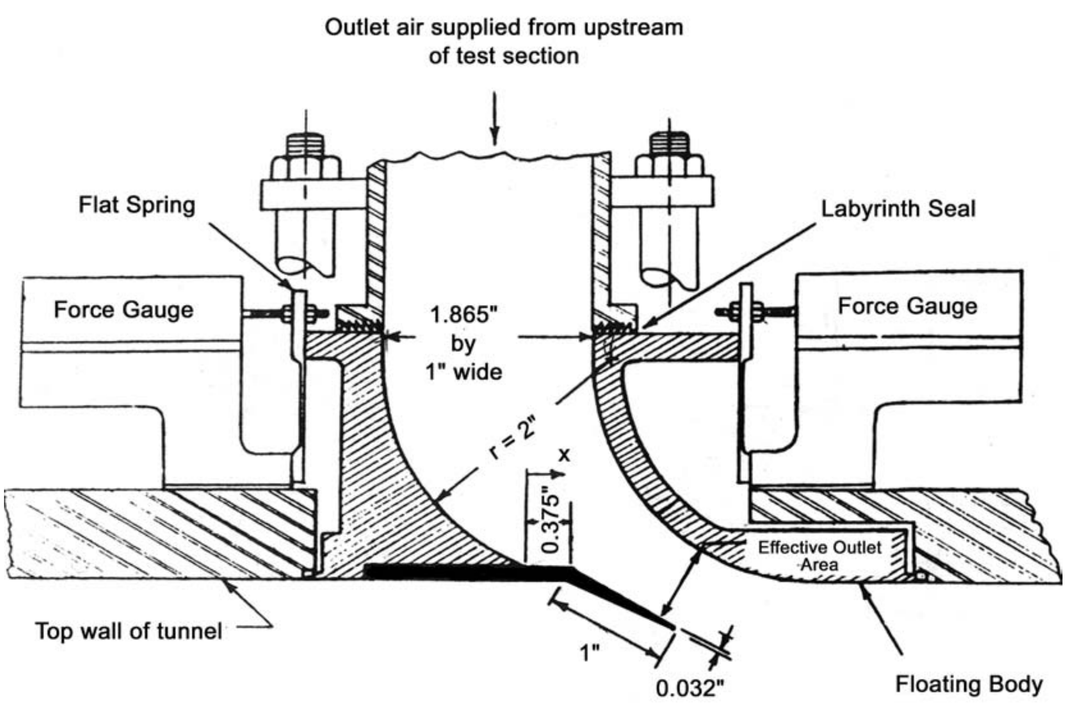


**Figure 1 :** Outlet geometry (adapted from NACA TN4007)

Flap angle is assumed to be fixed rather than freely hinged with flap weight considered negligible. By studying force data across a range of fixed angles it is possible to deduce hinge moments and therefore the steady state angle at which the flap will balance for a given pressure ratio and Mach number. The discharge characteristics for this flap angle can then be determined and therefore the performance of the outlet for given conditions. Meshes were created for flap angles from 15° to 45°, in 5° increments. The free-stream Mach number was varied from 0.4 to 0.85 in increments of 0.15. As a result, the ratio of leading edge boundary layer thickness to orifice length varied between 0.095 and 0.110.

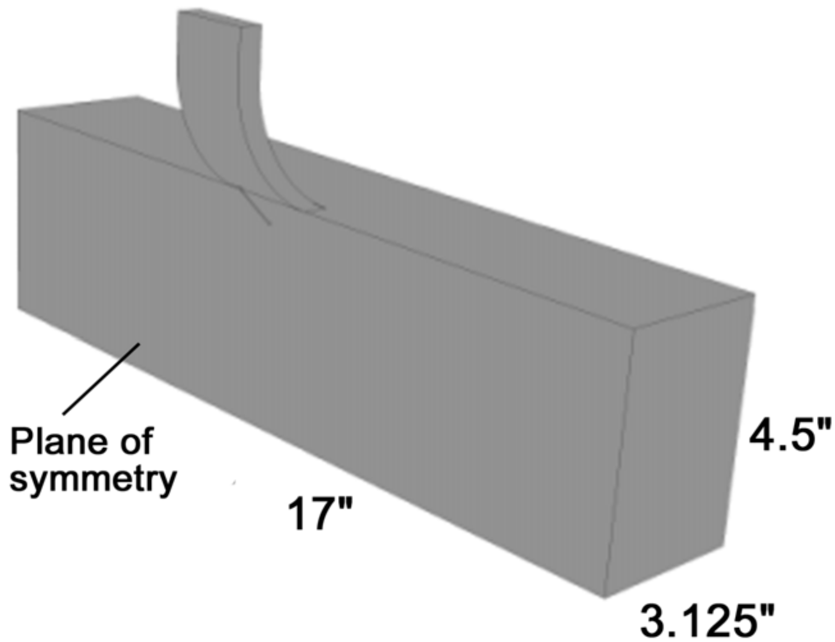


**Figure 2:** Computational domain

The performance of the duct is measured in terms of Discharge flow ratio (DFR) which is defined as the ratio of mass flow through the effective area of the orifice to the mass flow in the free stream through the same effective area as the orifice. The pressure ratio, defined as the ratio of duct total pressure to free stream total pressure, was varied between 0.64 and 0.97 in order to obtain the range of flow ratios required. Pressure inlet and outlet boundary conditions were applied and the realisable $k$-$\varepsilon$ turbulence model was used because of its known accuracy when dealing with flows involving jets, separations and secondary flows.

A mesh dependence study was performed to ensure that converged solutions were mesh independent.

## Results

Mass flow through the effective outlet area was extracted from the data files and discharge flow rates were calculated for each case, doubled to account for the symmetry plane. These values were plotted against angle for each pressure ratio and Mach number, as shown in figure 3. In each case the value of DFR increases with flap angle up to a maximum before falling off. The angle at which this maximum occurs decreases with increasing pressure ratio. Increasing Mach number also reduces the angle at which maximum discharge occurs. The maximum value of DFR increases with increasing pressure ratio but decreases with increasing Mach number.

Next the force on the flap, and load centre were extracted and used to calculate the moment about the hinge point for each case. These were converted to pitching moment coefficients by normalising with free-stream dynamic head, effective outlet area and flap length, with positive moment defined to be closing the flap. These values are then plotted against flap angle, shown in figure 4. Extrapolation of the data shows that for the majority of combinations of pressure ratio and Mach number, the zero pitching moment coefficients occurred in the range of $10^{o}$ to $15^{o}$. At lower pressure ratios and Mach numbers this point is lowered below $10^{o}$.

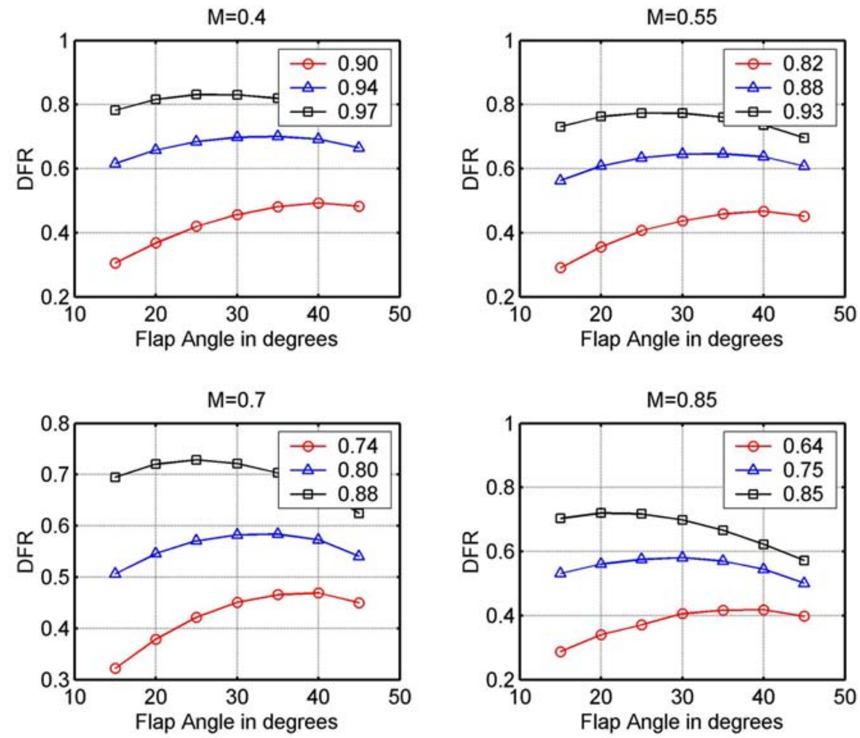


**Figure 3 :** DFR against Flap angle for a range of pressure ratios (legend) and angles

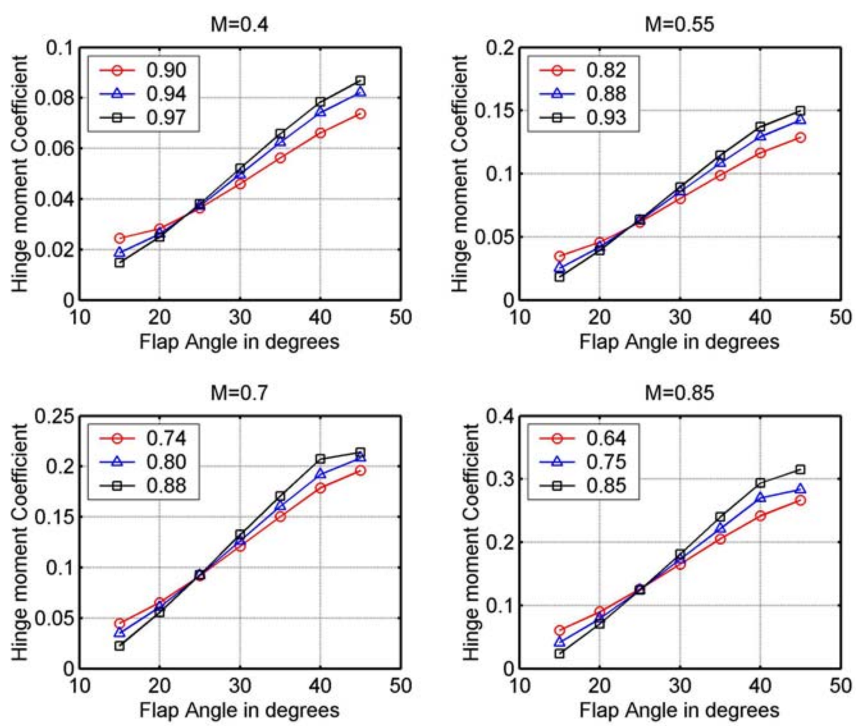


**Figure 4 :** Hinge moment coefficient against flap angle for a range of pressure ratios (legend) and Mach numbers

Increasing Mach number increases the hinge moments and curve gradients considerably. However for every pressure ratio and Mach number the curves intersect at a flap angle of $25^{o}$. For angles above this, increasing pressure ratio increases the pitching moment. Angles under $25^{o}$ show the opposite trend. There appears to be a maximum value for the moment as the curves begin to flatten at $45^{0}$, however more data at higher angles is required to verify this prediction.

To investigate the accuracy and validity of the CFD model, DFR and pressure ratio data were extracted from the plots in figure 3 for a single angle and plotted in figure 5 (dashed line) with the corresponding data from the NACA paper (solid line) across a range of Mach numbers. The curves through the CFD data points match the trend of the curves for the experimental data. However for a given pressure ratio the CFD result appears to under predict the DFR. This discrepancy increases with increasing pressure ratio with the effect becoming more severe with increasing free-stream Mach number. The maximum error at each Mach number increases from 5% at M=0.4 to 20% at M=0.85.

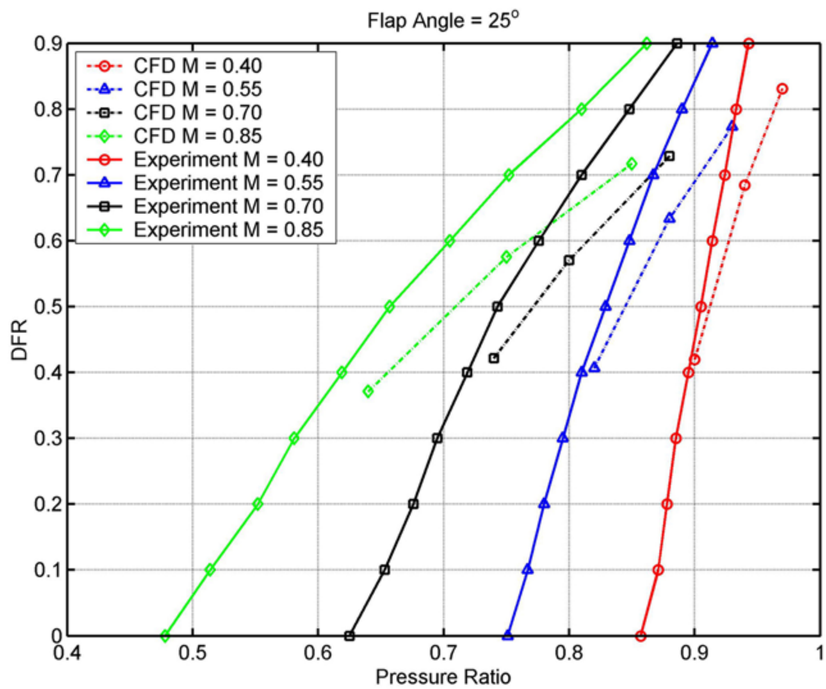


**Figure 5 :** DFR against pressure ratio, for flap angle=$25^{o}$, comparing NACA TN4007 and CFD results

The thrust generated by the outlet, defined positive in the stream-wise direction, was measured in the NACA paper through the use of a force gauge (see figure 1) and non-dimensionalised with free-stream dynamic head and effective outlet area. For comparison, the same thrust coefficient was calculated using the CFD results and taking into account the force on both the curved duct and flap. The envelope of thrust data from the NACA experiments is plotted in figure 6, along with the corresponding CFD data points, for a given flap angle. At lower values of DFR the predicted values of thrust fall within the envelope from the experimental data. At the larger values of DFR the CFD results over predict the generated thrust with the points lying just outside the envelope, with an error between 5% and 10%.

## Discussion

From the plots in figure 3 it can be clearly seen that flap angle has a pronounced effect on the discharge performance of the outlet. Previous studies[1,2] had indicated that flaps, or other protrusions, generated areas of low pressure over the outlet which increased discharge through suction. The mechanism behind this is the formation of a pair of longitudinal vortices, shed from the edges of the flap (c.f. a delta wing). As the flap angle increases the strength of the vortices increases until a maximum angle is reached. Beyond that angle the flap could be said to “stall” and behaves like a bluff body.

Figure 7 shows a series of plots of total pressure contours in the Y-Z plane of the computational domain, downstream of the outlet, for a flap angle of $15^0$, free-stream Mach number of 0.7 and pressure ratio of 0.8. Note that the symmetry plane has been plotted to illustrate the pair of vortices. The structure of the flow can be seen to develop downstream of the outlet as the vortices interact with the exhaust jet and shear layer shed from the trailing edge of the flap.

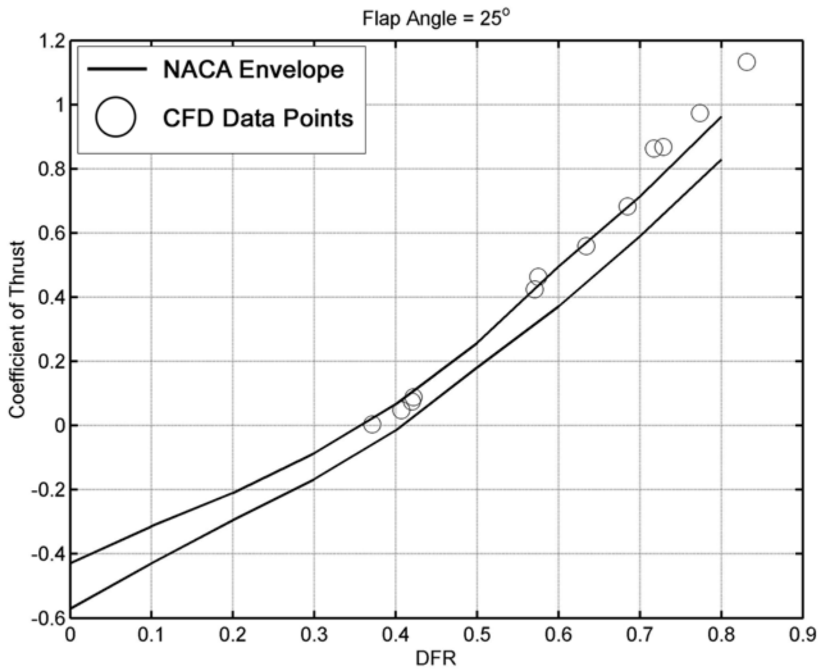


**Figure 6 :** Coefficient of thrust against DFR, for flap angle=25°, comparing NACA TN4007 and CFD results

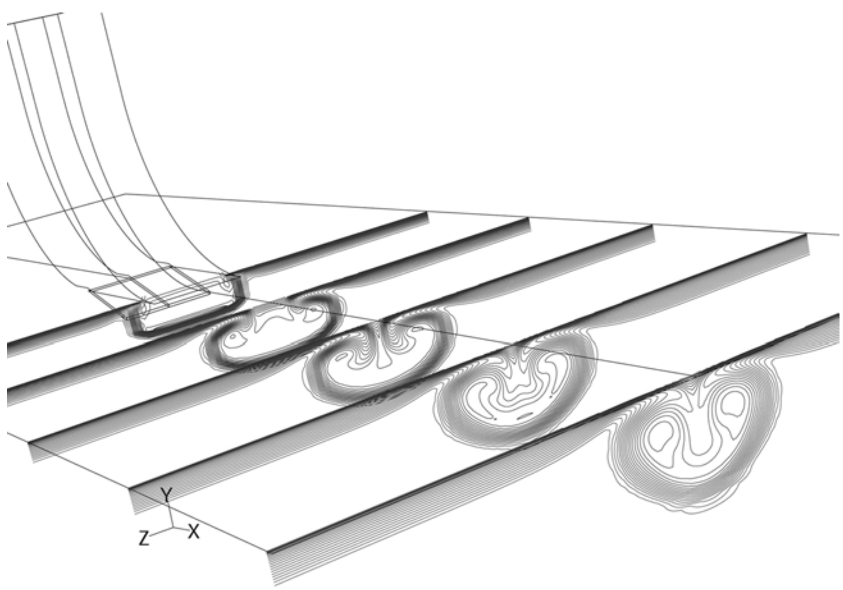


**Figure 7 :** Contours of total pressure, flap angle = 15°, M=0.7, pressure ratio = 0.8

Figure 8 shows a similar plot for a flap angle of 40$^o$ but with the same pressure ratio and free-stream Mach number, as shown in figure 8. A marked difference in the flow field can be seen, with a much stronger initial vortex pair leading to a larger flow structure further downstream. For the smaller flap angle, the flow structure impinges on the surface downstream which appears to have a thinning effect on the boundary layer in the downstream area outboard of the vortices.

Figure 8 however shows that for a large flap angle the structure is lifted away from the surface with the result that the boundary layer thinning does not occur, in fact, between the vortices the boundary layer is substantially thickened.

Variations in pressure ratio will change the nature of the discharge jet from the outlet, which will then in turn effect the manner in which the vortices, jet and shear layer interact. Free-stream Mach number will also determine the properties of the shed vortices and therefore the resulting flow structure. In cases of high Mach number and pressure ratio, flow in the outlet becomes choked as flow velocity exceeds sonic conditions and a normal shock is formed, as illustrated in figure 9. The position of this shock moves forward as the flap angle decreases, due to a repositioning of the throat of the outlet as effective area decreases.

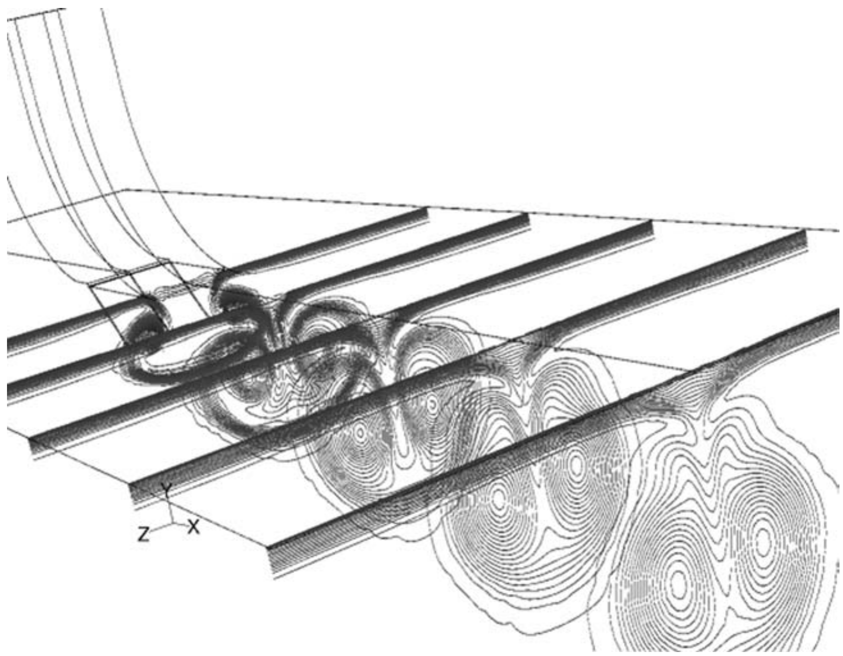


**Figure 8 :** Contours of total pressure, flap angle = 40$^o$, M=0.7, pressure ratio = 0.8

## Conclusions

Generally good agreement was achieved between the previously published data and the CFD prediction of integral properties such as DFR and thrust coefficient. Confidence has been gained that the numerical model, to a degree of accuracy, predicts the flow physics involved. A large amount of information is now available to be studied in an attempt to understand fluid mechanics involved. The numerical model can also be adapted to aid the design of a new experimental test rig, including the sizing of the required plenum chamber.

It is also noted that the information obtained may be of use in areas other than PRD design. A large number of engineering applications involve longitudinal vortices impinging on a surface, either from vortex generators or jets emerging into a cross flow. Such applications include boundary layer control, prevention of shock induced separation, cooling and chemical mixing. Through studying the flow structures around PRDs some insight into the interaction of longitudinal vortices and boundary layers may be obtained and applied to the applications mentioned above.

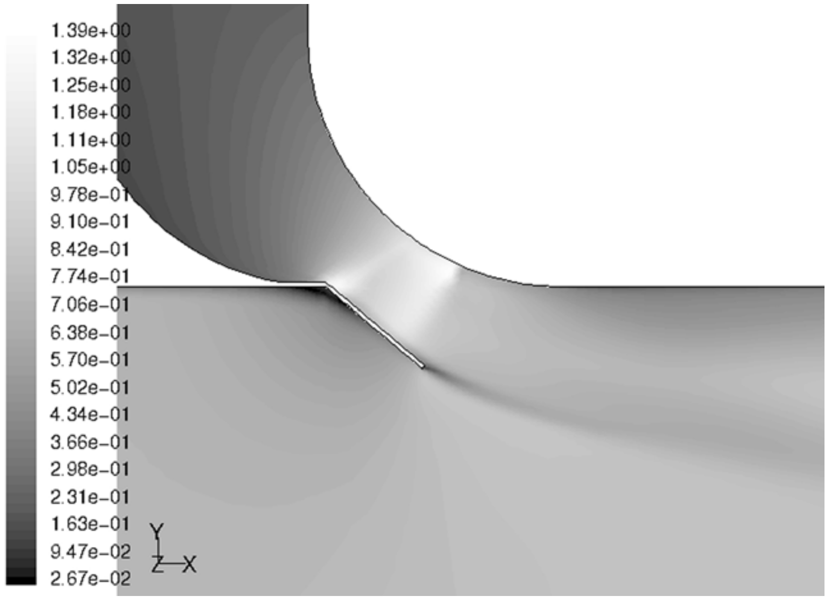


**Figure 9 :** Contours of Mach number, flap angle = 40$^{o}$, free-stream M=0.85, pressure ratio = 0.85

## Bibliography

1. Rogallo, F.M., *Internal-flow systems for Aircraft*, NACA, Report 713, 1941.
2. *Drag of Auxiliary Inlets and Outlets*, AGARD, 264.
3. Vick, A.R., *An Investigation of Discharge and Thrust Characteristics of Flapped Outlets for Stream Mach Numbers from 0.4 to 1.3*, NACA TN 4007, 1957.
4. Dewey, P., *A Preliminary Investigation of Aerodynamic Characteristics of Small Inclined Air Outlets at Transonic Mach Numbers,* NACA TN 3442, 1955.
5. Dewey, P. and Vick, A.R., *An Investigation of the Discharge and Drag Characteristics of Auxiliary Air Outlets Discharging into a Transonic Stream*, NACA TN 3466, 1955.